Research Square

Preprints are preliminary reports that have not undergone peer review.
They should not be considered conclusive, used to inform clinical practice,
or referenced by the media as validated information.

Hydrogeochemical and Isotopic Investigations on the Origins of Groundwater Salinization in Çarşamba Coastal Aquifer (North Turkey)

Abdourazakou MAMAN HASSAN
KTU: Karadeniz Teknik Universitesi
Arzu Ersoy (firat@ktu.edu.tr)
Karadeniz Technical University https://orcid.org/0000-0002-4181-1219

Research Article

Keywords: Hydrochemical Process, Stuyfzand Classification System, Seawater Intrusion, Çarşamba Coastal Aquifer, Turkey

Posted Date: August 23rd, 2021

DOI: https://doi.org/10.21203/rs.3.rs-388681/v1

License: This work is licensed under a Creative Commons Attribution 4.0 International License.
Read Full License

Version of Record: A version of this preprint was published at Environmental Earth Sciences on February 1st, 2022. See the published version at https://doi.org/10.1007/s12665-022-10248-5.

Abstract

The aim of this study is to determine the origins of salinization and the main hydrogeochemical process that controls the chemistry of Çarşamba coastal aquifer in Turkey. Therefore, a total of 33 groundwater samples and three seawater samples were analyzed in the coastal region of Çarşamba Plain in July 2019 and for these samples' physical parameters, major ions and environmental isotopes ($\delta^{18}O$, $\delta^{2}H$ and ^{3}H) values were determined. Piper, Chadha, Gibbs diagrams and Stuyfzand Classification Systems were used to determine the origins of salinization and the key hydrogeochemical process controlling the groundwater chemistry. According to Stuyfzand classification system, the study showed that the freshwater and fresh-brackish water main types are the most widespread in the study area. Six water subtypes were observed in the study area that include $CaHCO_3$, CaMix, NaMix, NaCl, $NaHCO_3$ and $MgHCO_3$. In addition, the subtypes CaMix indicated the locations of the transition zone, where the groundwater rich in Ca and HCO_3 and gradually enriched in Na changes from CaMix with HCO_3 as dominant anion to eventually CaCl and NaCl subtypes. Furthermore, the subtypes NaMix, $NaHCO_3$ and $MgHCO_3$ showed the locations of the transition zone where the flushing of the saline aquifer by freshwater takes place. All groundwater samples from study area had a positive cation exchange code and show that four hydrogeochemical facies composed of $CaHCO_3$; Ca-Mg-Cl and NaCl and $NaHCO_3$. Besides, groundwater samples have been influenced by two main mechanisms: the water-rock interaction and evaporation-crystallization. According to $\delta^{18}O$, $\delta^{2}H$ and ^{3}H analysis, the water samples have meteoric origin, shallow circulation, and a short residence time.

Introduction

Although many factors such as excessive pumping of groundwater, pollution, uncontrolled agricultural practices and industrialization lead to the depletion of the world water resources, salinization, especially in coastal aquifers, is the most important factors which pollutes groundwater resources. There are various potential sources of salinization of groundwater, such as natural saline groundwater, seawater intrusion, dissolution of halite, domestic, industrial and agricultural wastes. In the coastal area seawater intrusion is the principal source of salinization of groundwater, and very often requires the abandonment of wells in these zones (Al Farrah et al. 2011). Many research have been realized through the world to determine the sources of salinization of groundwater. The work carried out in Algeria by Djabri et al (2007) and in Ghana by Kortatsi (2006), based on the physicochemical analysis results of the water samples highlighted the influence of seawater intrusion and the dissolution of evaporate formations on the salinity of the coastal aquifers in their study area. In Syria Abou Zakhem et al (2006), using the results of physicochemical and isotopic analysis of the water samples taken from the north of Latakia and south of Tartous, demonstrated that salinization of groundwater in these coastal areas is mainly due to the mixing between freshwater and seawater; and that evaporation process has very limited effects. In France Veronique de Montey et al (2008) carried out research to evaluate different salinity sources of the confined aquifer of the Rhône delta by using chemical and isotopic groundwater compositions. According to the results of their study, seawater intrusion is the origin of increasing of Na,

thus promoting the process of exchange between Ca^{2+} and Na^{+}. In addition, this seawater intrusion also led to the reduction of SO_4^{2-} which is confirmed by the strongly depleted of $^{13}C_{TDIC}$ values.

In Turkey while the average annual rain precipitation in the world is around 1000 mm, the average precipitation is around 646 mm. This situation shows that Turkey in terms of water resources is not among the rich countries. In addition to the scarcity and uneven distribution of water resources, rapid population growth and pollution of water resources conduct to a further worsening of the water deficit (Toklu, 1999). On the other hand, unfavorable factors such as poor land use, urbanization and industrial organizations, wild storage areas, the discharge of untreated liquid waste into basins cause rapid pollution of surface and groundwater. Among the sources of water pollution in most coastal areas of Turkey, the salinization process is one of the most worrying factors, which mainly threatens groundwater resources. In general, in coastal areas the groundwater level decreases due to excessive pumping of groundwater. This excessive groundwater pumping lowers the level of the freshwater table and consequently reduces the pressure exerted by the freshwater column, which then allows the denser saltwater to move inland lateral (Barlow 2003). Arslan et al (2012), Fırat Ersoy at al (2020) and Fırat Ersoy at al (2021) carried out research to determine the influence of seawater on groundwater in the right bank of the Bafra Plain, by using the results of hydrochemical and isotopic analysis. According to the results of their study, some wells have very high EC, TDS, Cl^{-} and Na^{+} values, and the isotope distributions of $\delta^{18}O$ and $\delta^{2}H$ showed that all water samples were grouped around the freshwater-seawater mixing line. The work carried out in Van by Özler (2001) and in Mersin by Demirel (2014) based on the results of physicochemical analysis of groundwater samples taken in coastal area highlighted the influence of seawater intrusion due to excessive pumping of groundwater. According to the previous research that has been done in Çarşamba coastal aquifer, excessive increases of chloride, sodium, EC and TDS values were observed. Between 1990 and 2012, water quality in this zone was severely deteriorated due to the excessive pumping of groundwater and the resulting seawater intrusion (Arslan 2017).

This study seeks to determine the salinization origins and the main hydrogeochemical process controlling groundwater chemistry of Çarşamba coastal aquifer based on the results of physico-chemical and isotopic analyzes ($\delta^{2}H$, $\delta^{18}O$ and ^{3}H) of groundwater samples collected in this region. Due to its position on the Black Sea coast, Çarşamba plain is a region where intense agricultural activities take place. It is assumed that the excessive pumping of groundwater in this region for agricultural activities leads to contamination of the aquifer by the seawater intrusion. In addition, the excessive use of fertilizers, pesticides in agricultural areas as well as industrial wastes from the industrial areas leads to pollution of groundwater in this region. This study therefore made it possible to highlight the influence of seawater intrusion caused by the agricultural and industrial activities taking place in the study area on the groundwater chemistry in the Çarşamba aquifer.

General Properties and Geology

The study area is located on the left bank of the Yeşilırmak river and the western part of the Çarşamba plain, Turkey, lying between the latitudes 41° 11' 30" and 41° 16' 30" and the longitudes 36° 22' 00" and

36° 36' 00"; the plain of Çarşamba is situated in the Middle of Black Sea Region (Figure 1). The climate of this region is semi humid and the average annual precipitation is about 700 mm and the average annual temperature is about 17 ^{o}C (Arslan, 2014). The wet period is from October to the end of December.

There are three formation types in the study area, which are the Tertiary age Tekkeköy formation, Eocene age Sarıyurt formation and Quaternary age Alluvium formation (Figure 2). The Sarıyurt formation consists of sandstones, siltstones, marls and conglomerates. Its upper part is composed of interstratified siltstones, sandstones and marls while an alternation with sandstones is observed in the middle part. In the lower part of this formation, conglomerates and sandstones are observed. The Tekkeköy formation, consists of sandstones, mudstones, basalts, marls and tuffites alternation and agglomerates. The Quaternary Alluvium which covers almost the entire study area, consists of sands, gravels, clays, sandstones, muds and silts (**Yoldaş et al., 1985**). The geology of the study area indicates that only the Quaternary Alluvium can be considered as important groundwater reservoirs. The volcanic rocks of the Çarşamba plain are geological formations which have the characteristics of the secondary aquifer after the alluvial deposits in terms of groundwater. In these formations, the weathered basalts and in particular the interconnected cracks and the fracture systems developed in the agglomerate levels, facilitate transportation and accumulation of groundwater (**DSI, 1993**). The geological cross-section of study area is given in Figure 3. In terms of hydrogeological characteristics, the Çarşamba plain can be divided into two parts: the left bank and the right bank of the Yeşilırmak river. The left bank is generally composed of unconfined and semi-confined aquifers while on the right bank semi-confined and confined aquifers are the most frequent (**DSI, 1993**). On the left bank of Yeşilırmak river where the study area is located, the aquifer begins generally at a depth varying between 4 and 40 m and its thickness values ranged from 1 and 20 m. The majority of aquifers in the left bank of Yeşilırmak river consists of various layers of gravels, clayey-sands, clayey gravels and silty sands within the Quaternary alluvium. The aquifer of Çarşamba plain has available discharge between 2 and 32 l / s and a variable hydraulic gradient with a maximum value of 0.0025 (DSI, 1993; Arslan, 2014).

Materials And Methods

For this purpose, 33 groundwater samples and three seawater samples were taken in July 2019 in the study area. Groundwater samples were taken during the wet season from wells used in the study area for irrigation, industrial activities and domestic use. Water sampling was taken according to the TS EN ISO 5667 Water Quality Sampling standard (ISO,1991) defined in Turkish Standards. According to this standard, water sampling is done after 15 minutes of pumping in deep wells. Water samples were taken into polyethylene bottles pre-washed with pure water. For each sampling point the 1 L bottle was used for the major ion analysis and the 100 ml bottles were used for the minor ion analysis. For the analyzes of $\delta^{18}O$, $\delta^{2}H$ and ^{3}H, 1 L bottles were used. For these collected samples the physical parameters (TDS (Total Dissolved Solid), pH and EC (Electrical Conductivity)), major ions (SO_4^{2-}, CO_3^{-}, Cl^{-}, HCO_3, Mg^{2+}, Na^{+}, K^{+} Ca^{2+}), NH_4^{+}, NO_2^{-}, NO_3^{-} and environmental isotopes ($\delta^{18}O$, $\delta^{2}H$ and ^{3}H) values were determined. The global coordinates of all the sampling points expressed in the sexagesimal system were taken and recorded with a GPS device. The physical parameters of groundwater samples were determined in situ by

using HQD-Meter. The analysis and chemical parameters of groundwater samples were carried out at the Seventh Regional Directorate of Hydraulic works of the State (DSI) in accordance with TS EN ISO standards. The concentration of HCO_3^- and CO_3^- were determined by using titration method. Atomic absorption spectrometry TS EN ISO 14911 method were used to determine the concentrations of Na^+, Ca^{2+}, K^+, Mg^{2+} while NH_4^+. NO_2^-, NO_3^- SO_4^{2-} and Cl^- analysis were carried out by using ion chromatography method. The environmental isotopes ($\delta^{18}O$, δ^2H and ^3H) analysis were carried out at the Isotope Laboratories of the Technical Research-Quality Control Directorate of the State Hydraulic Works. The mass spectrometry method was used to determine the value of δ^2H and $\delta^{18}O$; and the values of ^3H was determined by using liquid scintillation method. For the analysis of ^{18}O and ^2H, the precision values are ± 0.15 ‰ and ± 2 ‰, respectively. In this study all maps were made by using ArcGIS software. The spatial distribution maps were produced by using inverse distance weighted (IDW) interpolation method.

Hydrochemical Interpretation Methods

In this study, the determination of the salinization origins and the hydrochemical process controlling the groundwater chemistry is mainly based on the classification of water types according to Stuyfzand and Chadha diagram (Chadha 1999). In addition, bivariate diagrams of major ions such as Na-Cl, K-Cl, Mg-Cl and SO4-Cl were also used in this study for to determine the influence of seawater intrusion on groundwater in the study area. Hydrochemical facies of water samples was classified basis on the dominant ions using the Piper diagram (Piper 1944). The diagram of Gibbs was used for to determine the main mechanisms controlling the groundwater chemistry in the study area. Groundwater chemistry is in general controlled by various mechanisms such as weathering of rocks, precipitation and evaporation. Thus, this diagram is constructed by plotting TDS on the Y-axis against Na / (Na + Ca) on the X-axis for cations; and TDS on the Y-axis against Cl / (Cl + HCO_3) on the X-axis for anions (Gibbs, 1970). Chadha diagram is used in general for the classification of natural waters as well as the identification of hydrochemical process. This diagram is constructed by plotting on the X axis the difference between alkaline earths and alkali metals (($Ca^{2++}Mg^{2+}$) – ($Na^{++}K^+$)) against weak acidic anions and strong acidic anions ((HCO_3^-+CO_3^{2-}) – (SO_4^{2-} + Cl^-)) on the Y axis, of water data expressed as milliequivalent percentage. The milliequivalent proportion differences from the axis X and Y are prolonged further into the principal study subfields of the proposed diagram, which defines the global character of water (Chadha, 1999). The $\delta^{18}O$, δ^2H and ^3H analyzes were carried out to determine the origin, the relative age of the groundwater and whether the seawater intrusion into the aquifer is significant in the study area. The groundwater origin and the mixing process between freshwater and seawater was determined by using the relationship between δ^2H and $\delta^{18}O$, Sinop Meteoric Water Line (D = 8* δ18O + 16.4) (Dilaver et al. 2018) and Global Meteoric Water Line (δ D = 8* δ18O + 10) (Craig 1961). In addition, to assess the seawater influence on groundwater the cross plot of Cl^- vs $\delta^{18}O$, EC vs $\delta^{18}O$, EC vs ^3H and Cl^- vs ^3H were used.

The Stuyfzand classification system was developed by Stuyfzand (1986) as a new system applied to aquifer systems by combining the characteristics of existing classification systems. This system had

been improved for the first time specifically for groundwater from coastal aquifers limestone systems with cation exchange phenomena caused by the intrusion of fresh or salt water. After the system has been extended for non-calcareous aquifer systems (Stuyfzand, 1985). Consequently, this classification can be applied for groundwater from all hydrogeological systems. This system, based on the determination of different types of water by subdividing the principal chemical characteristics of groundwater at 4 levels, is important in determining the principle of cation exchange in groundwater (Ersoy and Ersoy, 2008).

The first level of this classification of groundwater, which corresponds to the main type of water, is determined according to the chloride content. Therefore, depending on the chloride concentration, there are six different main types; fresh (F), fresh-brackish (Fb), brackish (B), brackish-salt (Bs), hyperhaline (H) and salt (S) (Stuyfzand, 1986; Ersoy and Ersoy, 2008). The classification of water main according to the Cl^- is given in Table 1. The second level that represents the water type is determined according to the hardness values. The classification of water types according to the hardness values is given in Table 1. The third level of this classification that corresponds to the subtype of water is determined according to the dominant anions and cations. However, it should be noted that in this classification, the cation or anion with most meq / l does not necessarily determine the name. The strongest hydrogeochemical family is first determined for both cations and anions, e.g. the families [Na+K+NH_4] and [SO_4+NO_3+NO_2]. The stronger member of the two families is then chosen to form the combination. The theoretical maximum number of subtypes is 54. However, only 16 subtypes have been discovered, namely those listed in Table 2. The class of water is finally determined according to the sum of Mg, K and Na in meq / l, adjusted for contribution of sea salt according to the following formula: $(K+ Mg+ Na)_{corrected} = (K+ Mg + Na)_{measured} - 1.061*Cl^-$. Where:

The symbol "-" often indicates the intrusion of salt water when $(Mg+K+Na)_{corrected} <- \sqrt{(0.5\ Cl)}$;

The symbol "+" often indicates freshwater encroachment when $(Mg + K+ Na)_{corrected} > \sqrt{(0.5Cl)}$ and

the symbol "ϕ" often indicates an equilibrium when $-\sqrt{(0.5\ Cl)} \leq (Mg + K+ Na)_{corrected} \leq \sqrt{(0.5\ Cl)}$.

The factor 1.061 of the previous formula corresponds to the ratio {(Mg + K + Na) / Cl} for the average seawater. It is also supposed that all chlorine ions come from the sea and the fractionation of the main components of seawater during spraying can be neglected and that the Cl concentration behaves conservatively (Stuyfzand, 1986). The water classification according to Stuyfzand classification system is given in Table 2.

Results And Discussion

Hydrochemical Parameters of Groundwater Samples

The pH values of groundwater samples are between 6.5 – 8, TDS values range is 2679.20 – 399.16 mg/l and EC range is 587 - 3940 µS/cm (Table 3). High values of EC and TDS were observed in wells located

towards the center, in the northeast part and locally in the west part of the study area while the lower values are observed in the northern part, towards the west and south part. Ca^{2+}, Mg^{2+}, Na^{+} and K^{+} values are respectively between 52.91 – 167.2 mg/l, 16.65 – 114.21 mg/l, 20.01 – 609.04 mg/ and 1.56 – 25.35 mg/l. The NH_4^{+} values range is 0 – 4.39 mg/l with a median value of 0.92 mg/l (Table 3). Higher Na^{+} value was observed in well number 13 located respectively in the center of the study area. Anion's analysis results show that the Cl^{-} values range is 18.08 – 1001.82 mg/l, HCO_3^{-} values range is 248.92 – 822.41 mg/l and SO_4^{2-} values range is 19.69 – 504.80 mg/l. The NO_3^{-} values range is 0.25 – 101.68 mg/l with a median value of 16.06 mg/l. High concentrations of NO_3 usually come from discharges of industrial wastewater, urban domestic wastewater, septic systems, human waste lagoons, feedlots and animal wastes as well as the use of nitrogen fertilizers in the study area. The high Cl^{-} values were observed towards the center, the western part and locally towards the northeast of the study area. It is observed that the high values of Cl^{-}, Na^{+}, TDS and EC have been observed in industrial and agricultural areas. These values indicate a seawater intrusion caused by an over-extraction of groundwater in these areas. The high NH_4^{+} values observed in some wells are influenced by industrial waste, the excessive use of fertilizers and pesticides in the study area.

Piper classification diagram showed four different water facies in the study area, which are $CaHCO_3$, Ca-Mg-Cl, NaCl and Ca-$NaHCO_3$ (Figure 4). The $CaHCO_3$ water type, which is dominant in the study area, represents around 73% of analyzed samples. The abundance in the study area of this water type that is characterized by the dominance of Ca and HCO_3 ions reveals a strong carbonate rock-water interaction and strong recharge process. The Ca-Mg-Cl water type represents 18% of analyzed samples and were observed in 22, 19, 33, 5, 7 and 14 wells number. The Ca-$NaHCO_3$ water types were observed in wells number 23 and 16 and represented around 6% of analyzed samples. NaCl water type is only observed in 13 well number. The Ca-$NaHCO_3$ water types of results from the cation exchange between seawater and fresh water during the freshening process. In addition, the presence of Ca-Mg-Cl and NaCl water facies indicates also the seawater intrusion in the study area.

The Piper diagram can also be used in determining of seawater intrusion into groundwater by using Kelly (1955) classification. So, on this diagram, the fresh groundwater samples will land near the area labeled "fresh water", while the water resulting from a conservative mixture (mixture without ion exchange reactions) between freshwater and seawater would be drawn along the line labeled "mixed water"(Kelly, 2005).

According to this classification (Figure 4), 75.76 %, 21.21 % and 3.03 % of the groundwater samples fall in freshwater water area, mixed water area and seawater intrusion area, respectively. The water samples which fall in mixed and seawater intrusion areas indicated the influence of seawater on groundwater in the study area.

According to Chadha diagram, four water facies were observed in the study area which are $CaHCO_3$, Ca-Mg-Cl, NaCl and $NaHCO_3$ (Figure 5). The $CaHCO_3$ water type that falls in field 5 of diagram is the most

widespread in the study area and represents around 70% of analyzed samples. This dominant water type reveals as in the piper diagram, that the weathering of host rocks and recharge process are most important in the study area. The Ca-Mg-Cl water type, which falls in field 6 of diagram, represents around 12% of analyzed samples and were observed in wells number 22, 7, 14 and 33. This water type indicates reverse ion exchange process that corresponds to the beginning of the salinization process in the study area. The Na-Cl water type, which falls in field 7 of diagram, represents around 9% of analyzed samples and were observed in wells number 13, 31 and 28. This water type indicates evaporation, mixing between freshwater, and seawater. The $CaNaHCO_3$ water type that falls in field 8 of diagram represents around 9% of analyzed samples and were observed in wells number 1, 16, 14 and 23. This water type shows the cation exchange reaction resulting from the flushing of the saline aquifer by freshwater.

Data plotted on Gibbs diagram show that in the study area groundwater are influenced by two main mechanisms that include water-rock interaction and evaporation-crystallization (Figure 6). The groundwater samples that fall in rock dominance field are the most widespread and represents around 80% of analyzed samples. The rock–water interaction, which is dominant, indicates that the in the study area local geological context and hydrogeological conditions significantly influence the chemical composition of groundwater. The groundwater samples that fall in evaporation-crystallization dominance field are the least dominant and represents around 20% of analyzed samples. These results also show that in addition to evaporation, the seawater intrusion into the aquifer influence the chemical composition of groundwater.

Bivariate diagrams of major ions such as Na-Cl, K-Cl, Mg-Cl and SO_4-Cl can be successfully used to investigate the origin of groundwater salinization (Telahigue et al; 2020). The Figure 7 indicates the bivariate diagrams of major ions and EC versus Cl of groundwater samples. According to this figure strong linear positive correlation was observed between Cl and Na (R = 0.9127) (Figure 7.a), moderate linear positive correlation between Cl and SO_4 (R = 0.583) (Figure 7.b), Cl and Mg (R = 0.5878) (Figure 7.c) and between Cl and EC (R = 0.761) (Figure 7.d). No significant correlation was observed between Cl and Ca (R = 0.0312) (Figure 7.f). The Strong linear positive correlation observed between Cl and Na indicates that these ions come from the common source which is seawater intrusion. The moderate correlation observed between Cl and EC shows also the influence of seawater on groundwater in the study area. In the coastal area the concentration of Cl and EC values are used as classic indicators of salinization of groundwater (El Moujabber et al; 2006). The bivariate diagram of Cl/HCO3 ratio and Cl is generally used to determine the mixing of groundwater and seawater (Seddique et al; 2019). According to this diagram, in the study area most of water samples that have lower Cl/HCO_3 ratios can be characterized as fresh waters (Figure 7.e). However, some water samples present high Cl/HCO_3 ration and high Cl values. These samples indicate so the mixing of groundwater and seawater in the study area. The moderate correlation observed between Cl and SO_4, Cl and Mg indicates also that some of these ions come from seawater. However, the majority of water samples do not follow the linear correlation line of the Cl-Mg and Cl-SO4 bivariate diagram which correspond to the fresh-seawater mixing line. This situation indicates other sources for the enrichment in Mg2+ and SO4 in the study area.

Stuyfzand Classification System

The spatial distribution of the first level of water classification according to Stuyfzand, which corresponds to the main type of water determined according to the chloride content, shows that the study area can be divided into three regions: the fresh, fresh-brackish and brackish-salt water regions (Figure 8). The freshwater, which represents 84,84% of the samples, occupies a very large portion of the study area. The fresh-brackish water represents around 9% of groundwater samples and occupies in the south, the center, north and northeast of the study area. This dominance of F and Fb can be explained by the significant recharge of the aquifer and the abundant infiltration of surface water, which contributes to the refreshing of aquifer and limits the mixing between salt and fresh water at least in the study area. The Bs water main type was only observed in one well located towards the center of the study area.

The spatial distribution of the second level of water classification, which corresponds to the type of water, determined according to the total hardness values, shows that the study area can be divided into 3 regions: hard, very hard and extremely hard water regions (Figure 9). The groundwater samples' hardness values varying between 21 and 85.55 °F with an average of 44.22 °F. The very hard water region is the most widespread in the study area and represents around 67% of analyzed samples. The hard water region occupies locally the northeast, the Northwest and a small part of the center and south of study area. The extremely hard water types were only observed in one well located toward the center of study area.

The determination of the third level of this classification which corresponds to the water subtypes determined according to the dominant anions and cations shows that the water samples are distributed according to six types of facies: the $CaHCO_3$ facies, which represents around 60.60% of samples, the CaMix facies which represents around 18.19% of the samples, the NaMix facies which represents around 6.06% of the samples, the NaCl facies which represents 3.03% of samples, the $CaNaHCO_3$ facies, which represents 9.09 % of samples and finally the $MgHCO_3$ facies which represents 3.03% of samples (Figure 10). The facies of water samples determined according to Stuyfzand classification system is given in Table 4.

The spatial distribution the water subtypes shows that the subtypes $CaHCO_3$ are widely distributed in the study area, the subtypes CaMix are found in the west and the center, the subtypes $NaHCO_3$ are found in the center and extreme northwest, the subtypes NaMix occupy locally the north and the east, the subtypes NaCl are found in the center and finally the subtypes $MgHCO_3$ are found in the extreme east part of study area (Figure 11).

The last level of this classification, which corresponds to the water class, was determined according to the sum of K, Na and Mg in meq / l, adjusted for the contribution of sea salt, shows that all groundwater samples have positive cation exchange code.

The subtype CaMix, which occupies the west, and the center of the study area shows the transition zone location, where the groundwater rich in Ca and HCO_3 and gradually enriched in Na, changes from CaMix with HCO_3 as dominant anion, to eventually CaCl and NaCl facies. This process corresponds to the beginning of the salinization process in this area. In the coastal areas cation exchange reaction is the mainly process which controls hydrochemical composition of groundwater affected by seawater interference. This subtype CaMix was observed in wells number 2, 5, 7, 14, 22 and 33. The subtype NaCl observed in well number 13 also indicates the seawater intrusion in aquifer. Freshwater is in general considered as an infiltrating rain, which has dissolved calcite, the water type in this situation is F-$CaHCO_3\phi$, while the seawater type is S-NaClϕ (Al Farrah et al. 2011). Therefore, in the study area the salinization process is mainly caused by seawater intrusion which reduces the quality of groundwater. In addition, the excessive use of fertilizers, pesticides in agricultural areas as well as industrial waste from the industrial area leads to pollution of groundwater in this region. During the salinization process, a cation exchange reaction takes place, resulting in a deficit of Na^+, Mg^{2+} and K^+ and an excess of Ca^{2+} according to the following chemical reaction:

$$[aCa]\text{-}X + bNa^+ + cK^+ + dMg^{2+} \Rightarrow aCa^{2+} + [bNa, cK, dMg]\text{-}X + aCa^{2+}$$

During this cation exchange reaction there is an adsorption of dominant Na^+, K^+ and Mg^{2+} ions and a release of Ca^{2+} ions, causing the move of water resulting from NaCl water type to the CaCl water type, which is characteristic of salinization process. This process is generally at the origin of formation of the $(Na + K + Mg)_{deficit}$ in groundwater. The process of salinization in groundwater can be represented as follows:

$$CaHCO_3\phi \Rightarrow CaCl^- \Rightarrow NaCl^- \Rightarrow NaCl\phi$$

$$F \Rightarrow Fb \Rightarrow B \Rightarrow Bs \Rightarrow S$$

It is observed that the classes of samples number 2, 5, 7, 14, 22 and 33 affected by seawater intrusion, present falsely positive cation exchange code. This false positive cation exchange code is not due to cation exchange but due to Mg^{2+} ions which dissolved from the carbonate rocks in the study area.

The subtypes NaMix, $NaHCO_3$ and $MgHCO_3$ observed in the study area, indicate the locations of the transition zone where the flushing of the saline aquifer by freshwater takes place. This process is observed when freshwater from coastal aquifers infiltrates into salt water, thus causing the following chemical reaction:

$$aCa^{2+} + [bNa, cK, dMg]\text{-}X + aCa^{2+} \Rightarrow [aCa]\text{-}X + bNa^+ + cK^+ + dMg^{2+}$$

During this cation exchange reaction resulting from the flushing of the saline aquifer by freshwater, there is an adsorption of Ca^{2+} ions and a release of Na^+, $Mg^{2+}$and K^+ ions, causing the formation of $NaHCO_3$ which is typical for freshening. The freshening process is generally at the origin of formation of the (Na +

$K + Mg)_{surplus}$ in groundwater. It is accepted that initial seawater conditions (SNaClϕ) dominated in the beginning of the process. Original seawater diluted gradually due to the recharge phenomena and then sea water conditions coming from S ended up F (Stuyfzand 1986). The cation exchanges that occur during the freshening process can also be schematized as follows (Suyfzand,1986; Fırat and Ersoy 2008):

$NaCl\phi \Rightarrow NaCl+ \Rightarrow NaHCO_3+ \Rightarrow MgHCO_3+ \Rightarrow CaHCO_3+ \Rightarrow CaHCO_3\phi$

$S \Rightarrow Bs \Rightarrow B \Rightarrow Fb \Rightarrow F$

It is observed also that the groundwater samples affected by freshening process in study area present a positive cation exchange code which is due essentially to cation exchange between fresh water and salt water.

The high Na values observed in some samples could also come from ion exchange between the clay particles and groundwater. This exchange takes place between the Na^+ ions of the clay particles and the Mg^{2+} and Ca^{2+} ions of the groundwater. These ion exchanges therefore lead to an increase in Na^+ ions and a decrease in Ca^{2+} and Mg^{2+} ions in groundwater (Şahinci, 1991).

Isotopic Signatures

In hydrogeological studies, the analysis of natural variations in the content of heavy isotopes of oxygen (^{18}O) and hydrogen (^{2}H) present in the structure of water is one of the methods used in the study of the origin and dynamics of groundwater and surface water. Due to the differences in the heavy isotope content generally observed between groundwater and seawater, the isotope content of groundwater mixed with seawater can be easily separated from the isotope content of meteoric water. In the study area $\delta^{18}O$ and $\delta^{2}H$ content in groundwater ranged from -8.89‰ to -7.21‰ and from -56.41‰ to -46.64‰ respectively. In the study area groundwater origin was determined by using Sinop Meteoric Water Line ($D = 8* \delta^{18}O + 16.4$) (Dilaver et al. 2018) and Global Meteoric Water Line ($\delta D = 8* \delta^{18}O + 10$) (Craig 1961). The relationship between $\delta^{2}H$ and $\delta^{18}O$ allows to understand the mixing process between freshwater and seawater (Nair et al 2015). The Figure 11 shows the relationship between stable isotopes $\delta^{2}H$ and $\delta^{18}O$ of groundwater and seawater. According to the isotope distributions of $\delta^{18}O$ and $\delta^{2}H$, all groundwater samples have meteoric origins (Figure 12). However, it is observed that the water samples taken from wells number 13, 14, 16, 19 and 26 have more positive $\delta^{18}O$ and $\delta^{2}H$ values than the other samples. More positive values of $\delta^{18}O$ and $\delta^{2}H$ indicate interference between seawater and groundwater in the study area.

To determine the level of seawater intrusion into groundwater, important information can be obtained by examining the relationships between isotope analysis results and physico-chemical analysis results. There are close relationships between the values of ^{18}O, Cl^-, SO_4^{2-} and EC of groundwater. In general, seawater intrusion in aquifer results in an increase in the $\delta^{18}O$, Cl^-, SO_4^{2-} and EC values of the

groundwater. Relatively high values of $\delta^{18}O$ (0 ‰) as well as high concentrations of Cl and TDS indicate seawater origins, while low values of $\delta^{18}O$ and low content of Cl and of TDS are characteristics of fresh groundwater origin (Wang and Jiao, 2012). In this study to assess the seawater influence on groundwater the cross plot of Cl^- vs $\delta^{18}O$ and EC vs $\delta^{18}O$ were used. According to the Figure 13, more positive $\delta^{18}O$ values are observed in samples with higher Cl^- and EC values. Well number 13 with the highest values of Cl^- and EC also has the highest value of $\delta^{18}O$. In addition, high Cl^- and EC values and more positive $\delta^{18}O$ values are observed in well numbers 14, 28 and 22. The high values of $\delta^{18}O$, EC and Cl^- observed in these wells indicate the influence of seawater intrusion into groundwater.

Because tritium element is a radioactive isotope that degrades over time, it is present in low value in water with long residence time and high value in water with a short residence time. Due to this situation, the concentration of tritium in young water is higher than in olds water. In the study area groundwater values for ^3H ranged from 0.96 TU to 7.15 Tu. In this study to assess the seawater influence on groundwater, the cross plot of EC vs ^3H and Cl^- vs ^3H were also used. According to Figure 14, the groundwater samples from wells number 15, 14 and 32 have lower tritium content (< 3 TU) than the water samples from other wells. Therefore, these wells were recharged by groundwater having a longer transit time than that of groundwater which recharged the other wells. In addition, although the water samples from wells 15 and 32 have low tritium values, its EC (<1500 µS / cm) and Cl^- (< 4 meq / l) values are also low. This situation indicates that these wells are not affected by seawater intrusion. High values of EC (> 1500 µS / cm) and Cl^- (> 6 meq / l) were observed in wells 13, 28 and 22 due to seawater intrusion. The majority of the groundwater samples collected from study area have tritium values greater than 4 TU. In addition, it is found that most of these wells have EC values less than 1500 µS / cm and Cl^- values lower than 6 meq/l. The high values of ^3H indicate that these wells were recharged by water from recent precipitation.

Conclusion

This study seeks to determine the determined the hydrochemical properties of the groundwater of Çarşamba coastal aquifer; one of the most important coastal aquifers in Turkey. According to the first level of Stuyfzand groundwater classification the most widespread main types are freshwater and fresh-brackish water in the study area with respectively 84.84 and 9% of analyzed samples. However, brackish-salt water main type was observed in one water sample from well number 13. The second level of this classification showed that very hard water region is the most widespread in the study area and represents around 67% analyzed water samples. In addition, the third level of Stuyfzand groundwater classification showed that water samples were distributed into six types of facies, which are $CaHCO_3$, CaMix, NaMix, NaCl, $NaHCO_3$ and $MgHCO_3$. Piper diagram indicated that in the study area the hydrogeochemical facies of water samples are $CaHCO_3$, Ca-Mg-Cl, NaCl and Ca-$NaHCO_3$. Furthermore, Chadha diagram revealed four chemically different groundwater facies in the study area. These facies include $CaHCO_3$ that reveals the weathering of host rocks and recharge process; Ca-Mg-Cl and NaCl that indicated reverse ion

exchange process and $NaHCO_3$, which indicated the cation exchange reaction, resulted from the flushing of salt water by freshwater. Gibbs diagram showed that the groundwater samples are influenced by two main mechanisms that include water-rock interaction and evaporation-crystallization. The rock–water interaction is dominant and indicates that the local geological context and hydrogeological conditions significantly influence the chemical composition of groundwater. Groundwater values for $\delta^{18}O$, $\delta^{2}H$ and ^{3}H ranged from -8.89‰ to -7.21‰, from -56.41 ‰ to -46.64 ‰ and from 0.96 TU to 7.15 TU respectively. The isotope distributions of $\delta\ ^{18}O$ and $\delta\ ^{2}H$ showed that all groundwater samples have meteoric origins. According to the cross plots of Cl^- vs $\delta^{18}O$ and EC vs $\delta^{18}O$, more positive $\delta^{18}O$ values are observed in samples with higher Cl and EC values. High Cl^- and EC values and more positive $\delta^{18}O$ values are observed in well numbers 13, 14, 28 and 22. These wells were affected by seawater intrusion and the ^{3}H values indicated that more water samples have shallow circulation and a short residence time.

Declarations

Acknowledgements

The authors gratefully acknowledge scientific research project of Karadeniz Technical University, which supported this study under project Number 8168. The authors also thank the Directorate of 7th Region of State Hydraulic Works (DSİ, Samsun) which support was essential for the success of this research.

References

Abou Zakhem B, Hafez R (2007) Environmental isotope study of seawater intrusion in the coastal aquifer (Syria). Environmental Geology 51(8):1329-1339. https://doi.org/10.1007/s00254-006-0431-x

Al Farrah, N, Martens, K, Walraevens, K (2011) Hydrochemistry of the upper miocene-pliocene-quaternary aquifer complex of Jifarah plain, NW-Libya. Geologica Belgica 14(3-4): 159-174.

Arslan H, Cemek B, Demir Y (2012) Determination of seawater intrusion via hydrochemicals and isotopes in Bafra Plain, Turkey. Water resources management 26(13):3907-3922. https://doi.org/10.1007/s11269-012-0112-3

Arslan, H (2014) Estimation of spatial distrubition of groundwater level and risky areas of seawater intrusion on the coastal region in Çarşamba Plain, Turkey, using different interpolation methods. Environmental monitoring and assessment 186(8): 5123-5134. https://doi.org/10.1007/s10661-014-3764-z

Arslan H (2017) Determination of temporal and spatial variability of groundwater irrigation quality using geostatistical techniques on the coastal aquifer of Çarşamba Plain, Turkey, from 1990 to 2012. Environmental Earth Sciences 76(1): 38. https://doi.org/10.1007/s12665-016-6375-x

Barlow P M (2003) Ground water in freshwater-saltwater environments of the Atlantic coast (Vol. 1262). Geological Survey (USGS).

Chadha D K (1999) A proposed new diagram for geochemical classification of natural waters and interpretation of chemical data. Hydrogeology journal 7(5):431-439. https://doi.org/10.1007/s100400050216

Craig H (1961) Isotopic variations in meteoric waters. Science 133(3465): 1702-1703.

De Montety V, Radakovitch O, Vallet-Coulomb C, Blavoux B, Hermitte D, Valles V (2008) Origin of groundwater salinity and hydrogeochemical processes in a confined coastal aquifer: case of the Rhône delta. Applied Geochemistry 23(8): 2337-2349. https://doi.org/10.1016/j.apgeochem.2008.03.011

Demirel Z (2004) The history and evaluation of saltwater intrusion into a coastal aquifer in Mersin, Turkey. Journal of environmental management 70(3): 275-282. https://doi.org/10.1016/j.jenvman.2003.12.007

Devlet Su İşleri (1993) Çarşamba Ovası Hidrojeolojik Etüd Rapor (Turkish language).

Dilaver AT, Aydın B, Özyurt NN, Bayarı CS (2018) Türkiye Yağışlarının İzotop İçerikleri (2012-2016) Devlet Su İşleri Genel Müdürlüğü-Teknik Araştırma ve Kalite Kontrol Dairesi Başkanlığı ve Meteoroloji Genel Müdürlüğü-Araştırma Dairesi Başkanlığı, Ankara, Türkiye.

Djabri L, Rouabhia A, Hani A, Lamouroux C, Pulido-Bosch A (2008) Origin of water salinity in a lake and coastal aquifer system. Environmental geology 54(3): 565-573. https://doi.org/10.1007/s00254-007-0851-2

DSI (1993) Çarşamba Ovası Hidrojeolojik Etüd Raporu. Samsun: DSİ (in Turkish).

El Moujabber M, Samra BB, Darwish T, Atallah T (2006) Comparison of different indicators for groundwater contamination by seawater intrusion on the Lebanese coast. Water Resources Management 20(2): 161-180.

Fırat Ersoy A, Ersoy H (2009) Hydrogeochemical Modelling System: A Case Study of Gümüşhaciköy (Amasya, TURKEY) Aquifer. Fen ve Mühendislik Bilimleri Dergisi 3(2):267-284.

Fırat Ersoy A, Ayyıldız Turan N, Yıldız Özgül H (2020) Kızılırmak Delta Kıyı Alanındaki Tuzlanma Sürecinin Stuyfzand Modelleme Sistemi ile Değerlendirilmesi. Gümüşhane Üniversitesi Fen Bilimleri Enstitüsü Dergisi 10 (4): 949-960 (in Turkish).

Fırat Ersoy A, Ayyıldız Turan N, Arslan H, Kuleyin A (2021) Assessment of Seawater Intrusion in Kızılırmak Delta Coastal Area (North Turkey) Using Hydrochemical and Isotopic Data. Environmental Earth Sciences 80 (400).

Gattacceca JC, Vallet-Coulomb C, Mayer A, Claude C, Radakovitch O, Conchetto E, Hamelin B (2009) Isotopic and geochemical characterization of salinization in the shallow aquifers of a reclaimed subsiding zone: the southern Venice Lagoon coastland. Journal of Hydrology 378 (1-2):46-61. https://doi.org/10.1016/j.jhydrol.2009.09.005

Gibbs, R. J. (1970). Mechanisms controlling world water chemistry. Science 170(3962):1088-1090. https://doi.org/10.1126/science.170.3962.1088

Güngör A, Arslan H (2016) Assessment of water quality in drainage canals of Çarşamba plain, Turkey, through water quality indexes and graphical methods. Global Nest Journal 18(1):67-78.

ISO (1991) ISO 5667-2, 1991. Water Quality—Sampling. Part 2: Guidance on sampling techniques. International Organization for Standardization.

Kelly F (2005) Seawater intrusion topic paper. Island Country Health Department.

Kortatsi B K (2006) Hydrochemical characterization of groundwater in the Accra plains of Ghana. Environmental Geology 50(3):299-311. https://doi.org/10.1007/s00254-006-0206-4

Nair I S, Rajaveni S P, Schneider M, Elango L (2015) Geochemical and isotopic signatures for the identification of seawater intrusion in an alluvial aquifer. Journal of Earth System Science 124(6):1281-1291. https://doi.org/10.1007/s12040-015-0600-y

Ozler H M (2001, April) Active saltwater encroachment (from Lake Van) in the Van aquifer, East Turkey. In First International Conference on Saltwater Intrusion and Coastal Aquifers–Monitoring, Modeling and Management. Essaouira, Morocco

Piper AM (1944) A graphical procedure in the geochemical interpretation of water analysis. Trans Am Geophys Union 25:914–923

Seddique AA, Masuda H, Anma R, Bhattacharya P, Yokoo Y, Shimizu Y (2019) Hydrogeochemical and isotopic signatures for the identification of seawater intrusion in the paleobeach aquifer of Cox's Bazar city and its surrounding area, south-east Bangladesh. Groundwater for Sustainable Development 9: 100215

Stuyfzand PJ (1986) A new hydrogeochemical classification of watertypes: Principles and application to the coastal dunes aquifer system of the Netherlands. Proceedings, 9th Salt Water Intrusion Meeting, Delft. pp 641–656

Stuyfzand P J (1989) A new hydrochemical classification of water types. Iahs Publ 182:89-98.

Şahinci Ali (1991) Doğal suların jeokimyası. Reform Matbaası, Izmir.

Telahigue F, Mejri H, Mansouri B, Souid F, Agoubi B, Chahlaoui A, Kharroubi A (2020) Assessing seawater intrusion in arid and semi-arid Mediterranean coastal aquifers using geochemical approaches. Physics and Chemistry of the Earth, Parts A/B/C 115: 102811.

Toklu, Vefa, Hukuk (1999) Su Sorunu Uluslararası. Turhan Kitabevi, Türkiye.

Wang Y, Jiao J J (2012) Origin of groundwater salinity and hydrogeochemical processes in the confined Quaternary aquifer of the Pearl River Delta, China. Journal of Hydrology 438: 112-124. https://doi.org/10.1016/j.jhydrol.2012.03.008

Yoldaş R, Balkıray K, Granit S, Korkmaz S, Didik S, Kalkan İ, Ağrıdağ DS, Besbelli B (1985) Samsun ve dolayının (Kızılırmak-Yeşilırmak arasındaki bölgenin) jeolojisi ve petrol olanaklarına ilişkin rapor, MTA Rapor No 8130. (Turkish language)

Tables

Table 1: Water type and main type classification according to Stuyfzand Classification System (Stuyfzand, 1986)

Water Type		
Type	Cod	Total Hardness (F0)
Very soft	x	< 5
Soft	0	(5- 10)
Moderately hard	1	(10 - 20)
Hard	2	20 - 40
Very Hard	3	40 - 80
Extremely hard	4	80 - 160
Extremely hard	5	160 - 320
Extremely hard	6	320 - 640
Extremely hard	7	640 - 1280
Extremely hard	8	1280 - 2560
Extremely hard	9	> 2560
Water main type		
Main type	Cod	Cl (mg/l)
Fresh	F	< 150
Fresh-Brackish	Fb	150 - 300
Brakish	B	300 - 1000
Brakish-Salt	Bs	1000 - 10000
Salt	S	10000 - 20000
Hyperhaline	H	> 20000

Table 2: Water classification according to Stuyfzand Classification System (Stuyfzand, 1986)

Name	Subdivisions	Criteria	Codes
Water Main type	6	Cl	Fb, F, Bs, B, H and S
Water Type	11	Total hardness	X, 0, 1, 2, 3, 4, 5, 6, 7, 8, 9
Water Subtype	54	Most important cation and anion	NaCl, NaMix, KNO_3, CaCl, $CaSO_4$, $CaNO_3$, $NaHCO_3$, $CaHCO_3$, CaMix, MgCl, MgMix, $MgHCO_3$, $AlSO_4$, NH_4SO_4, $NaSO_4$, $FeSO_4$
Water Class	3	(Mg+K+Na) corrected for sea salt	-, +, ϕ

Where: Fb = Fresh brackish, F = Fresh, Bs = Brackish saline, B = Brackish, H= Hyperhaline S = Saline and

Table 3: Physico-chemical parameters, $\delta^{18}O$, $\delta^{2}H$ and ^{3}H values of groundwater samples

Parameters	Min	Max	Median
Ca (mg/l)	52.91	186.77	115.38
Mg (mg/l)	16.65	114.21	37.52
Na (mg/l)	20.01	609.04	107.05
K (mg/l)	1.56	25.35	7.15
NH4	0	4.39	0.92
Cl (mg/l)	18.08	1001.82	114.91
HCO_3 (mg/l)	248.92	822.41	471.26
SO_4 (mg/l)	19.69	504.8	132.11
NO3	0.25	101.68	16.06
pH	6.55	8	7.22
TDS (mg/l)	399.16	2679.2	852.33
EC (µS/cm)	587	3940	1253.42
$\delta^{18}O$ (‰)	-8.89	-7.21	-8.39
$\delta^{2}H$ (‰)	-56.41	-46.64	-52.52
^{3}H (TU)	0.96	7.15	4.68

Table 4: Types of water according to Stuyfzand classification system

Well number	Types of water	Well number	Types of water	Well number	Types of water
1	F2-$NaHCO_3$+	12	F2-$CaHCO_3$+	23	F2-$NaHCO_3$+
2	F3-CaMix+	13	B_s4-NaCl+	24	F3-$CaHCO_3$+
3	F2-$CaHCO_3$+	14	F_b3-CaMix+	25	F3-$CaHCO_3$+
4	F2-$CaHCO_3$+	15	F2-$CaHCO_3$+	26	F3-$MgHCO_3$+
5	F3-CaMix+	16	F2-$NaHCO_3$+	27	F3-$CaHCO_3$+
6	F3-$CaHCO_3$+	17	F3-$CaHCO_3$+	28	B_s3-NaMix+
7	F3-CaMix+	18	F3-$CaHCO_3$+	29	F2-$CaHCO_3$+
8	F3-$CaHCO_3$+	19	F2-$CaHCO_3$+	30	F2-$CaHCO_3$+
9	F3-$CaHCO_3$+	20	F3-$CaHCO_3$+	31	F_b3-NaMix+
10	F3-$CaHCO_3$+	21	F3-$CaHCO_3$+	32	F3-$CaHCO_3$+
11	F3-$CaHCO_3$+	22	F_b3-CaMix+	33	F3-CaMix+

Figures

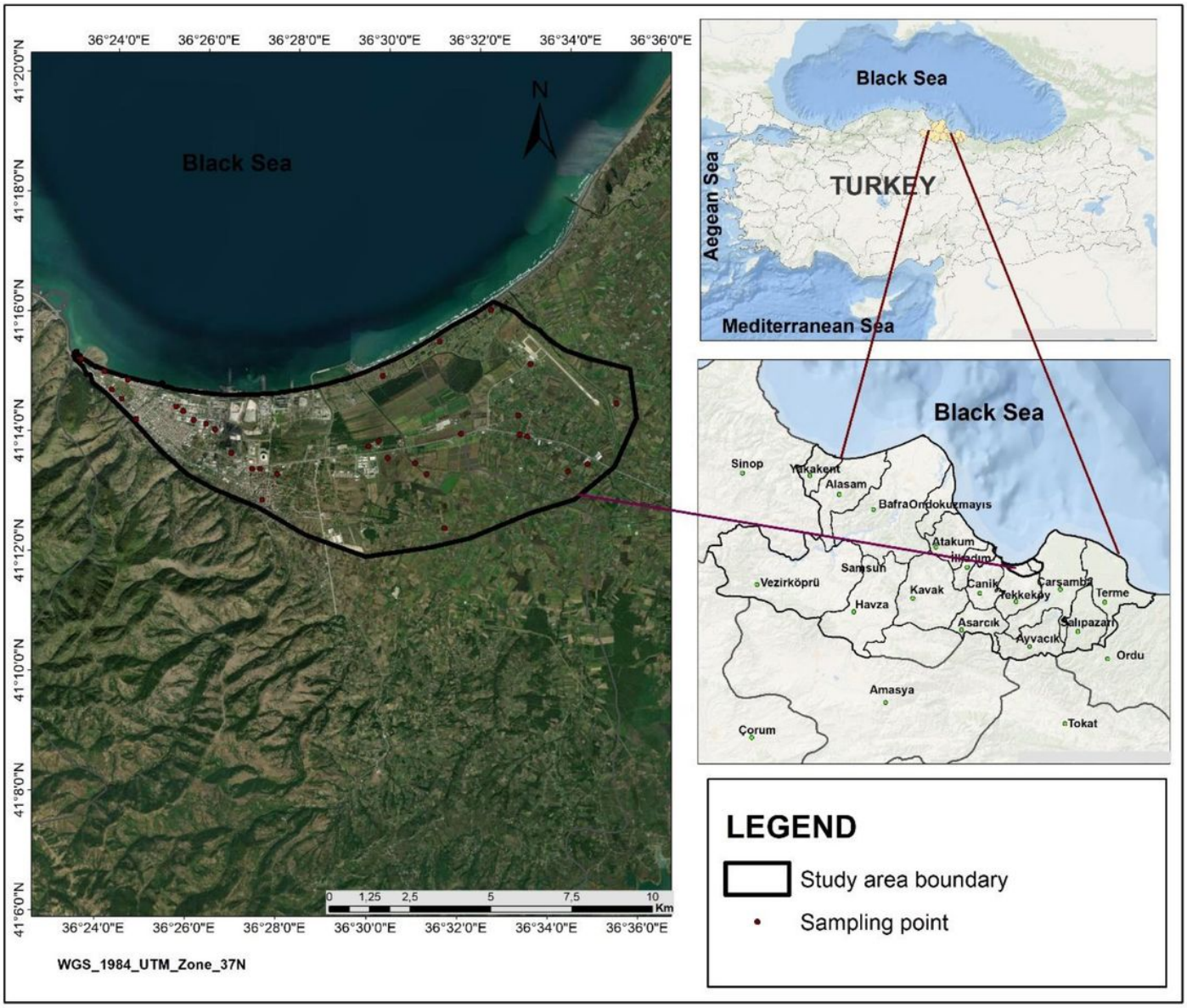


Figure 1

Location map of the Çarşamba Coastal Aquifer (Samsun-NE Turkey)

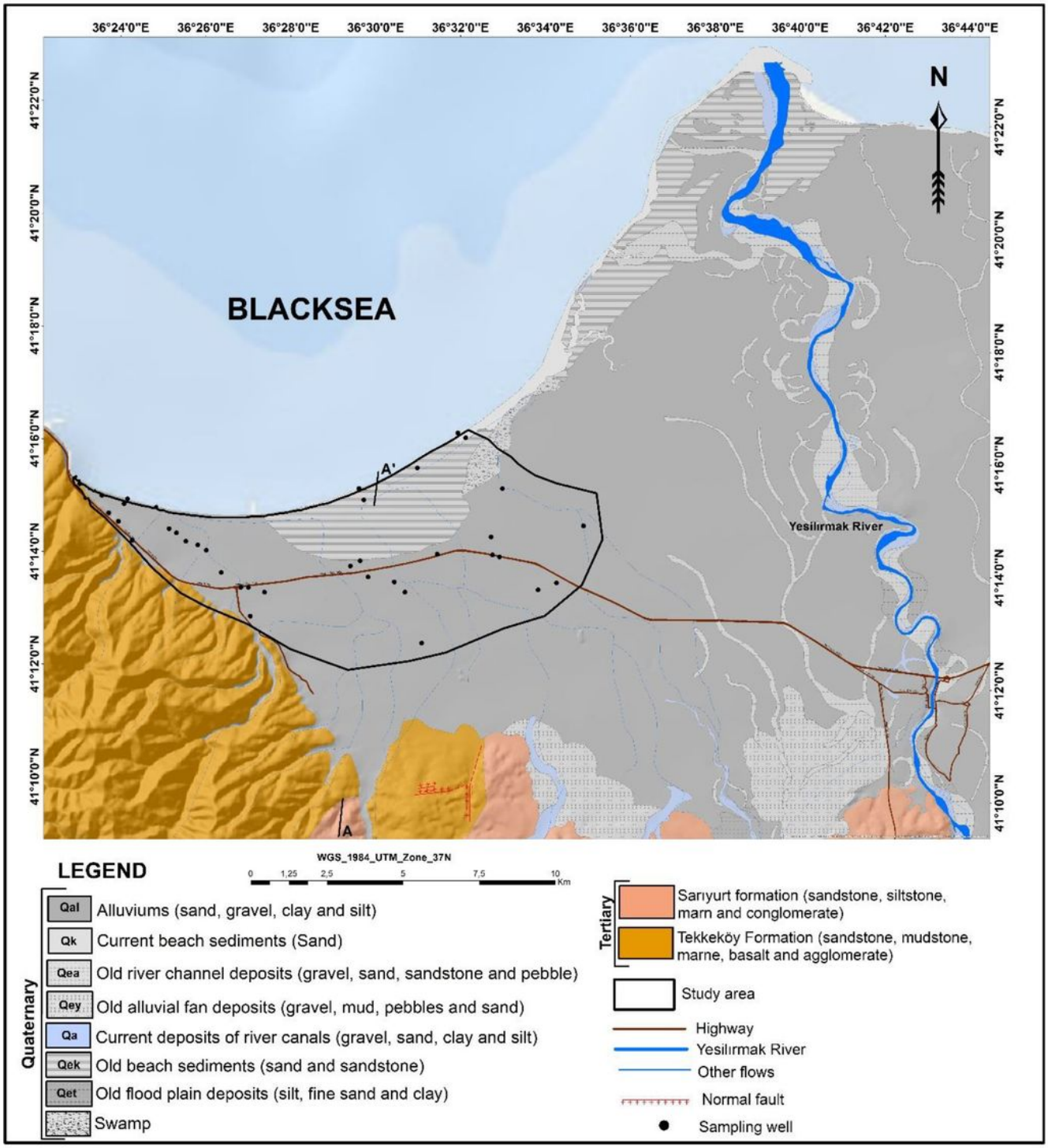


Figure 2

Geological map of Çarşamba Coastal Aquifer

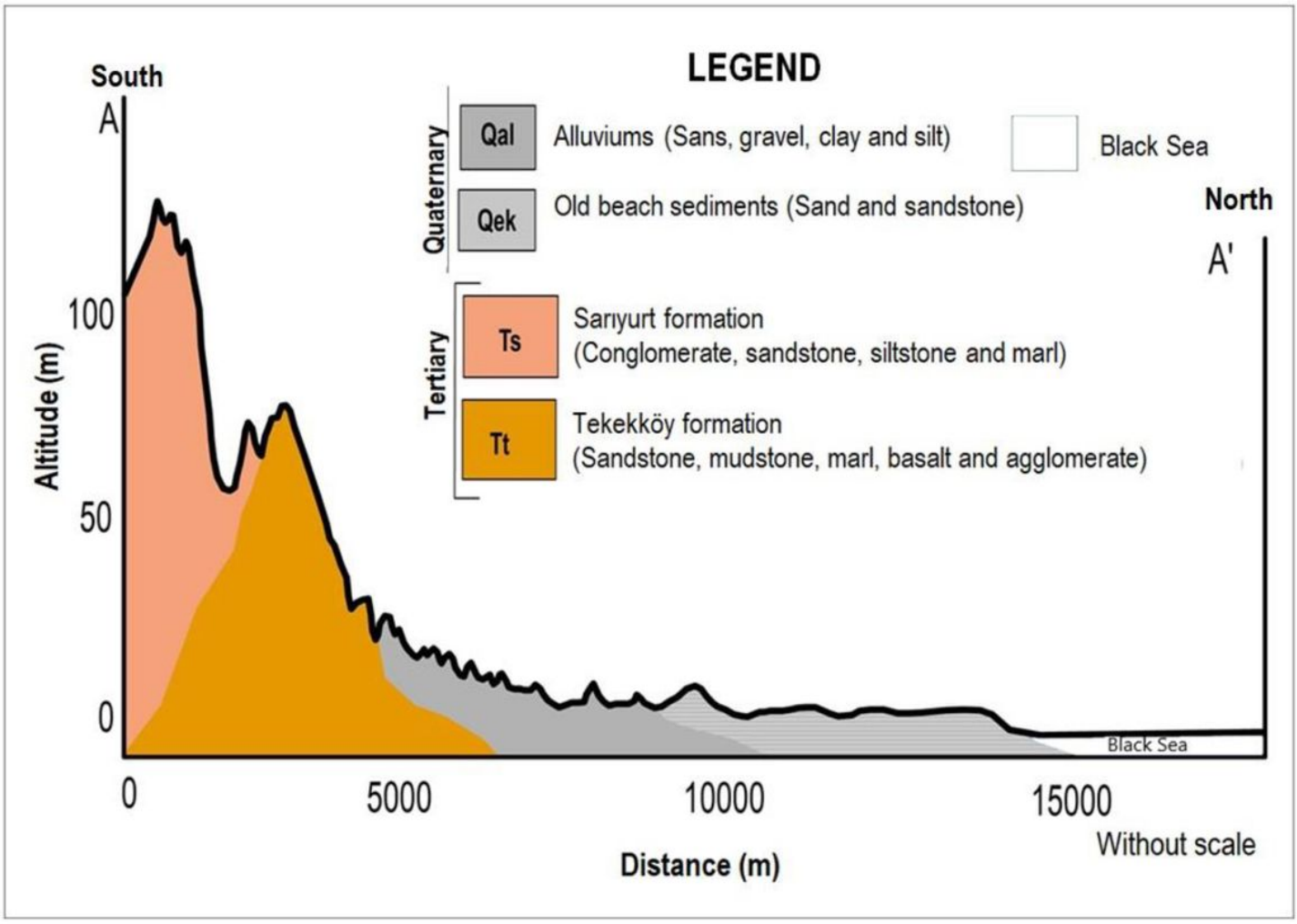


Figure 3

The geological cross-section of the study area

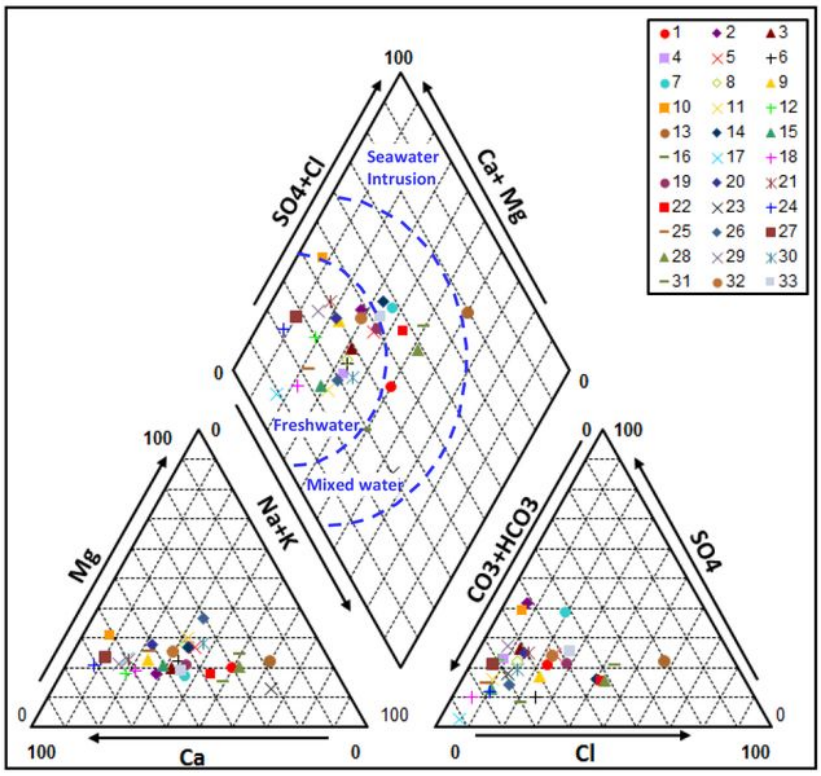


Figure 4

Groundwater types according to Piper diagram

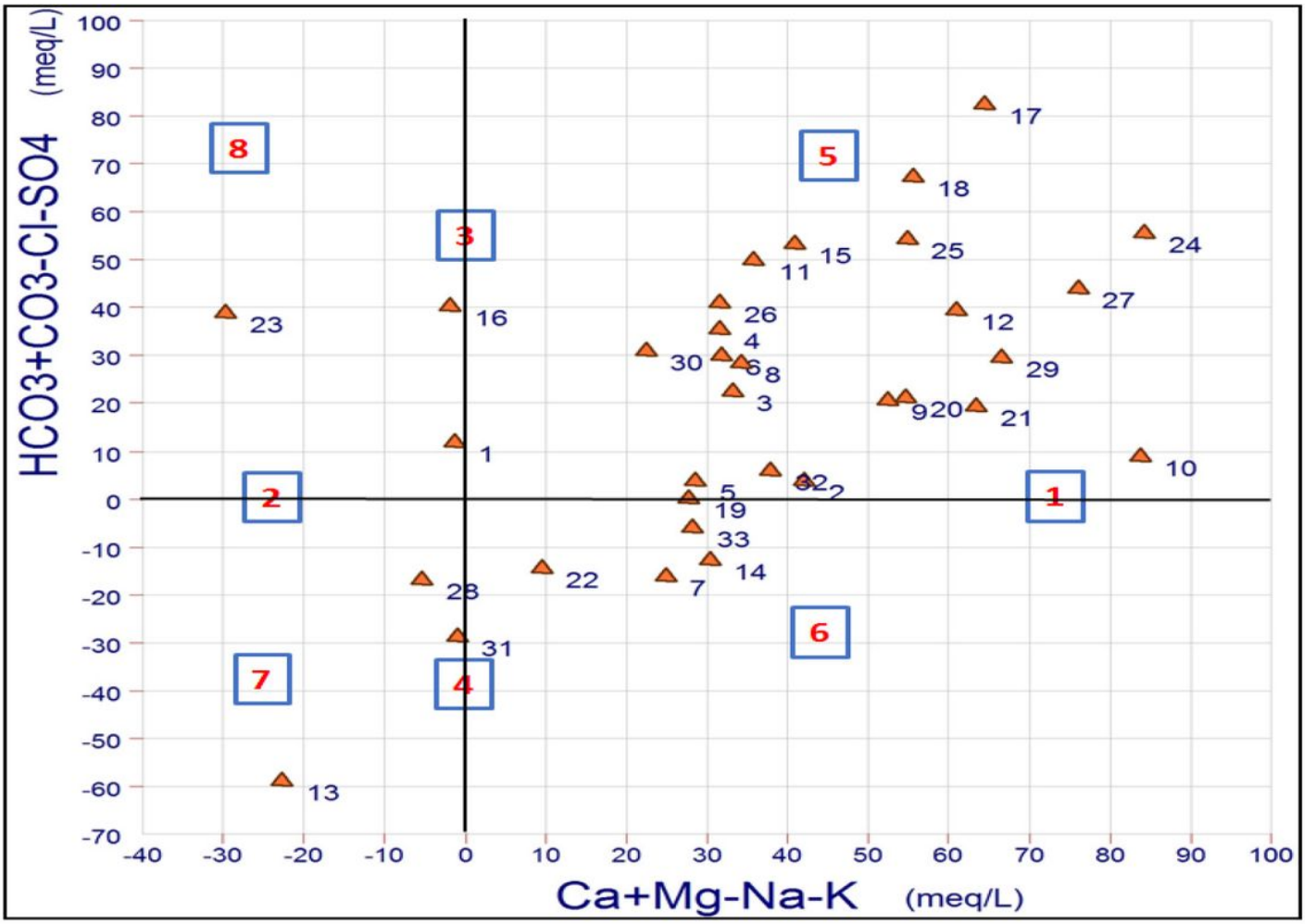


Figure 5

Groundwater types according to Chadha diagram

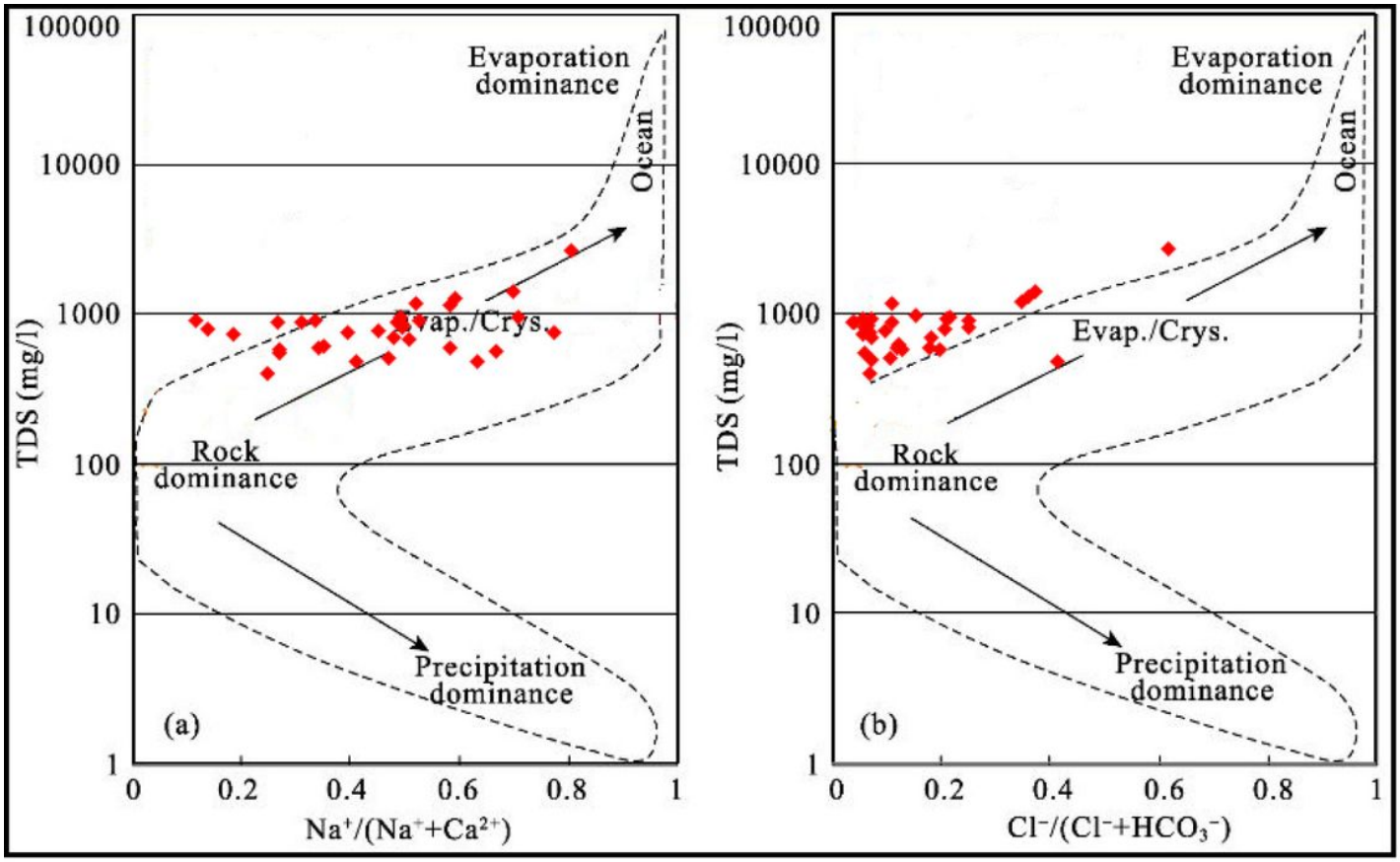


Figure 6

Gibbs diagram

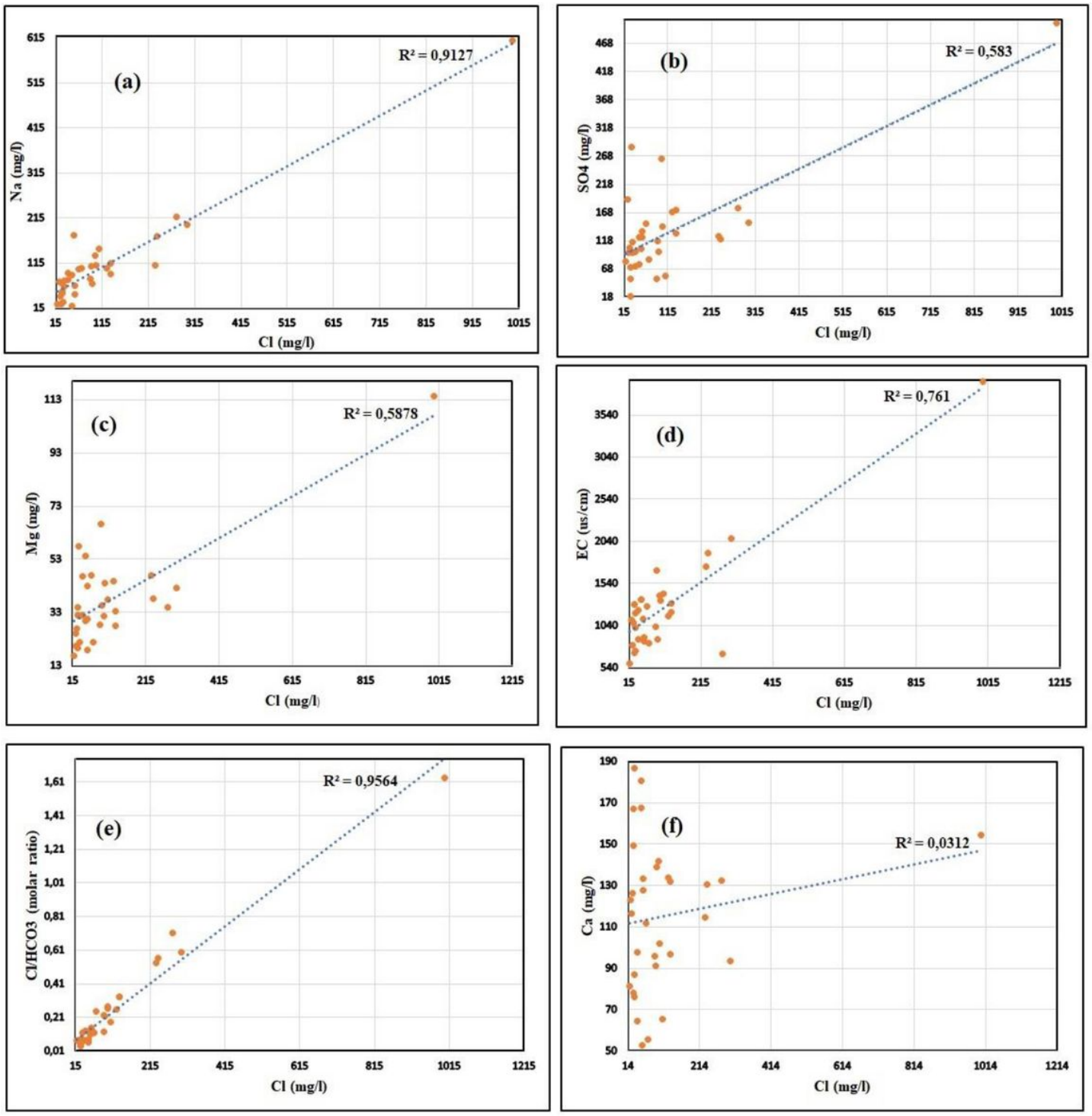


Figure 7

Relationship between Cl and Na (a), Cl and SO4 (b), Cl and Mg (c), Cl and EC (d), Cl and Cl/HCO3 (e) and Cl and Ca (f) of water samples

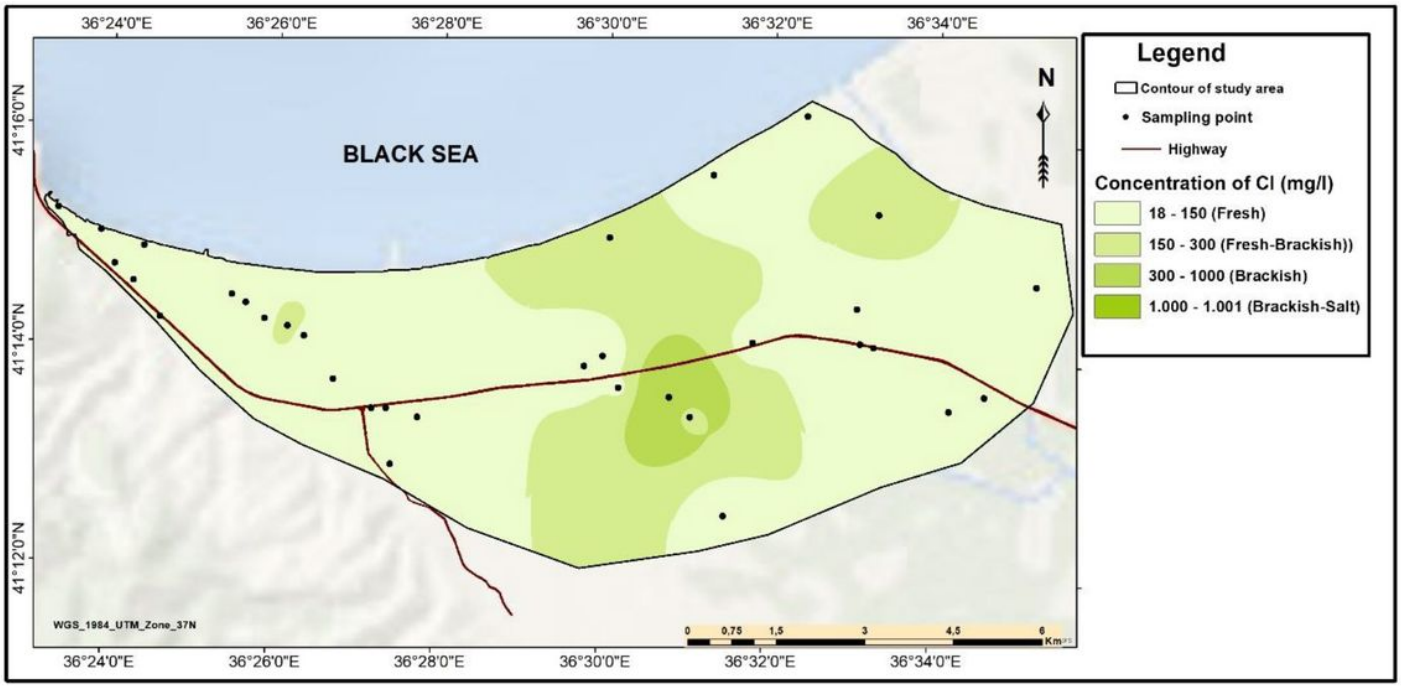


Figure 8

Distribution of water main type

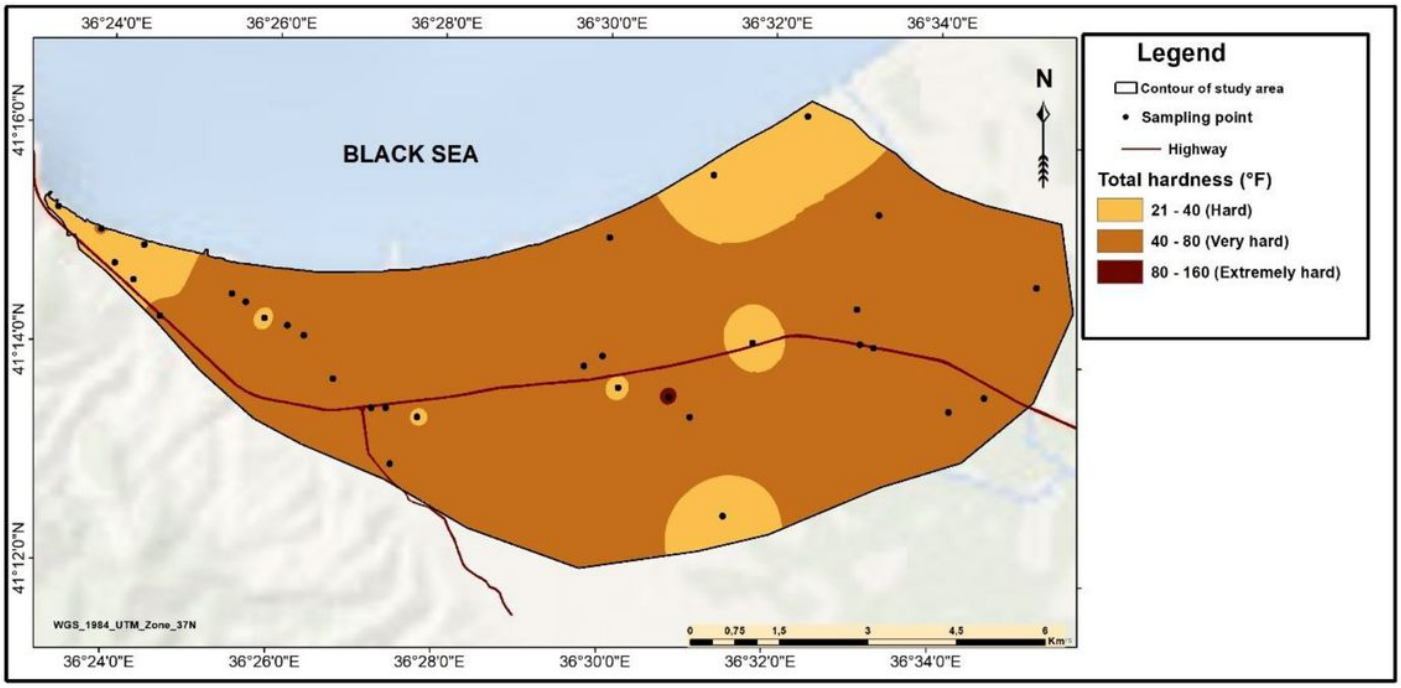


Figure 9

Distribution of water type

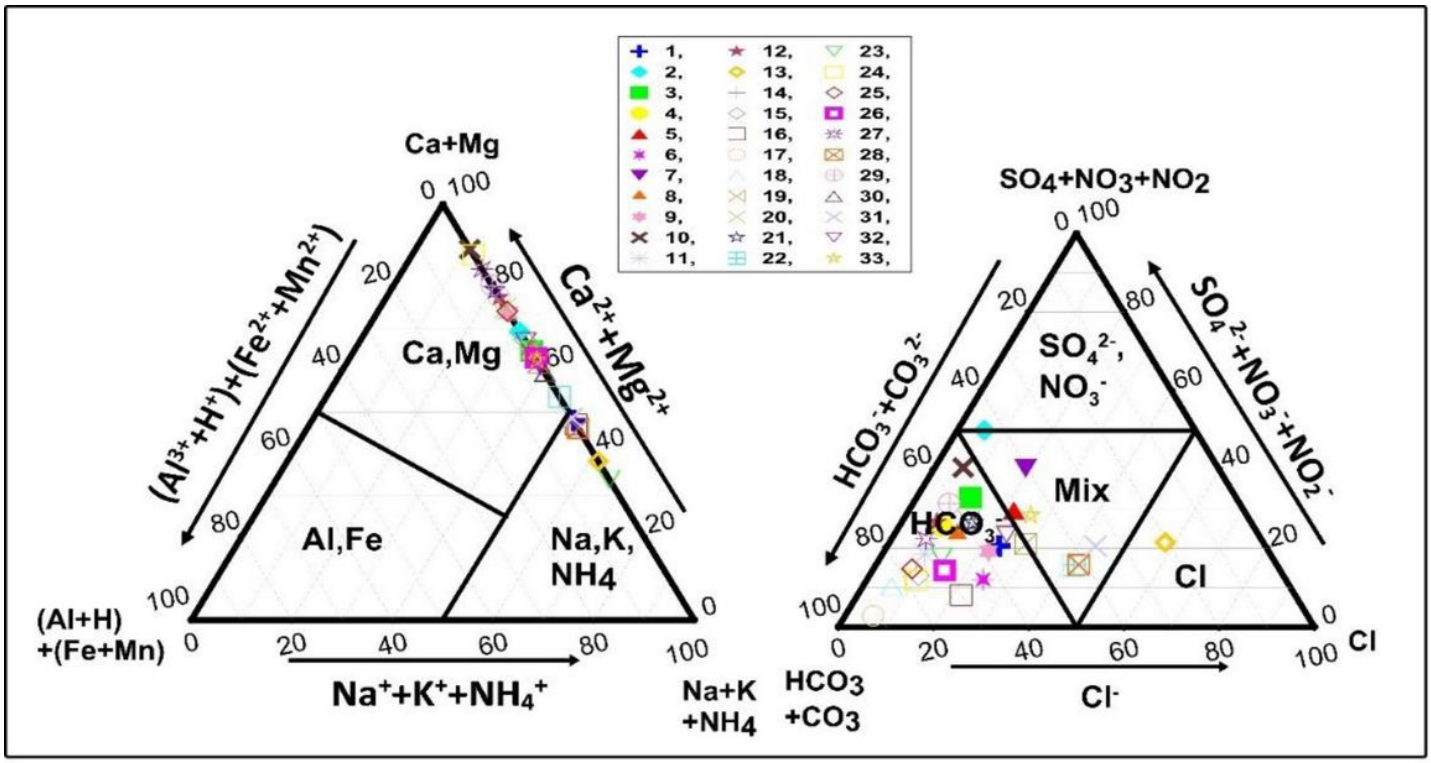


Figure 10

Water subtypes according to Stuyfzand Classification System

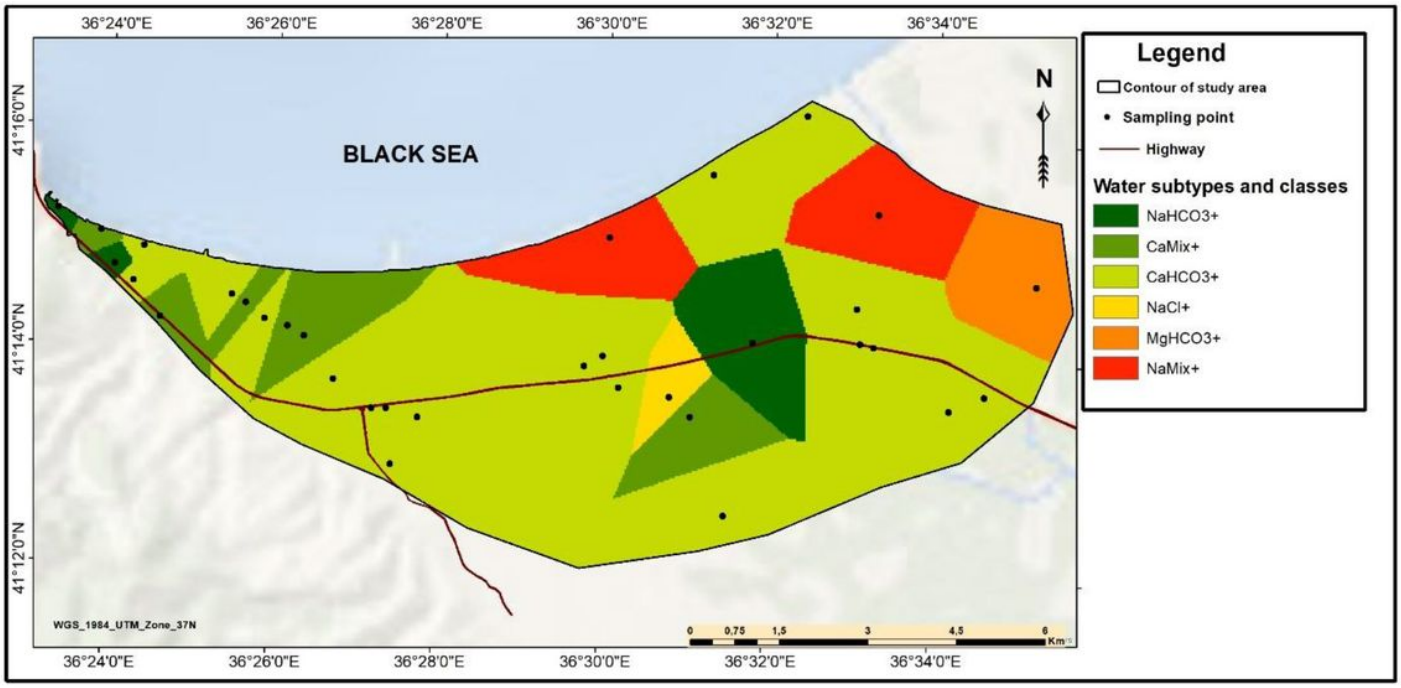


Figure 11

Distribution of water subtypes and classes

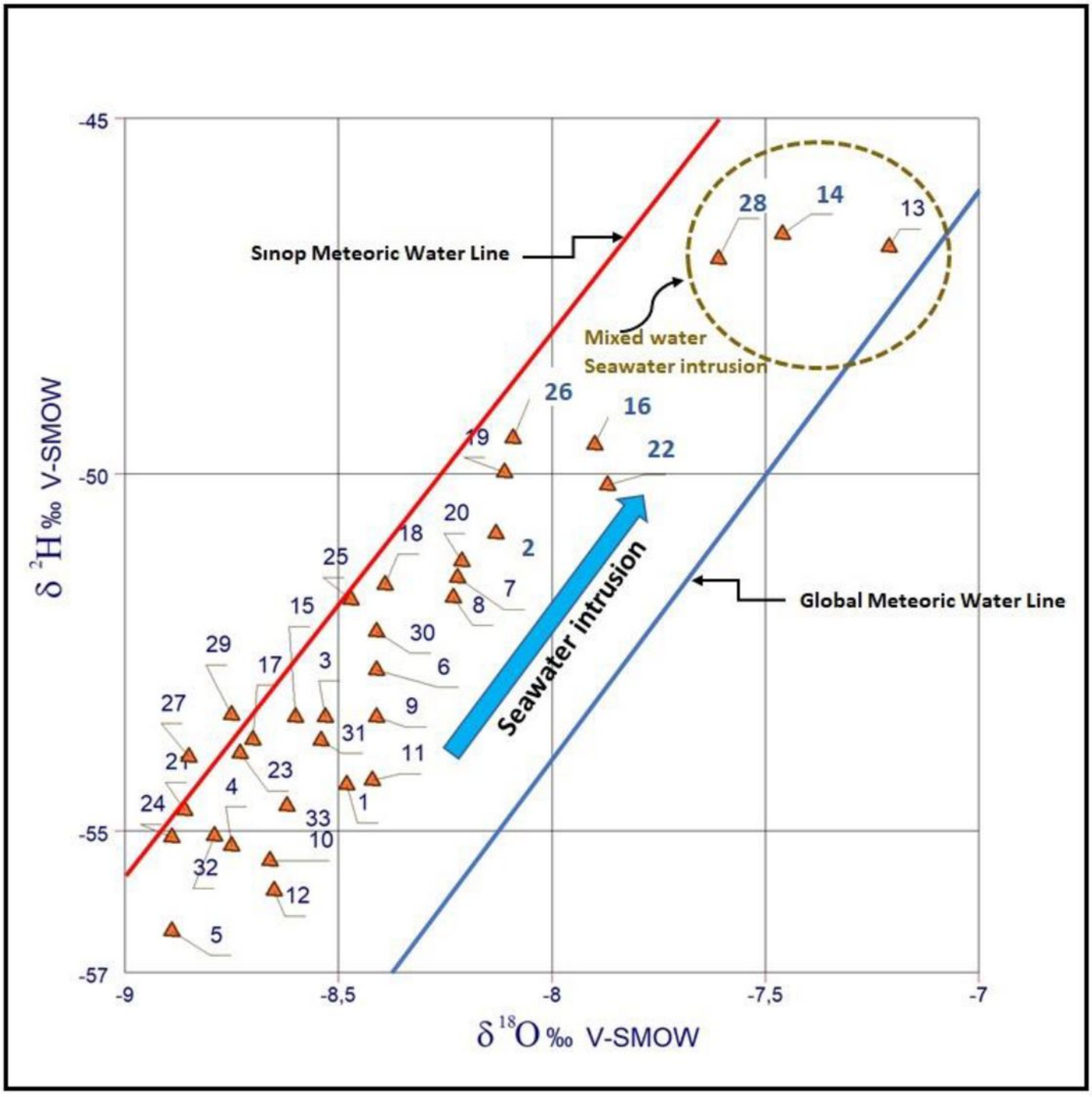


Figure 12

Relationship between δ18O and δ2H

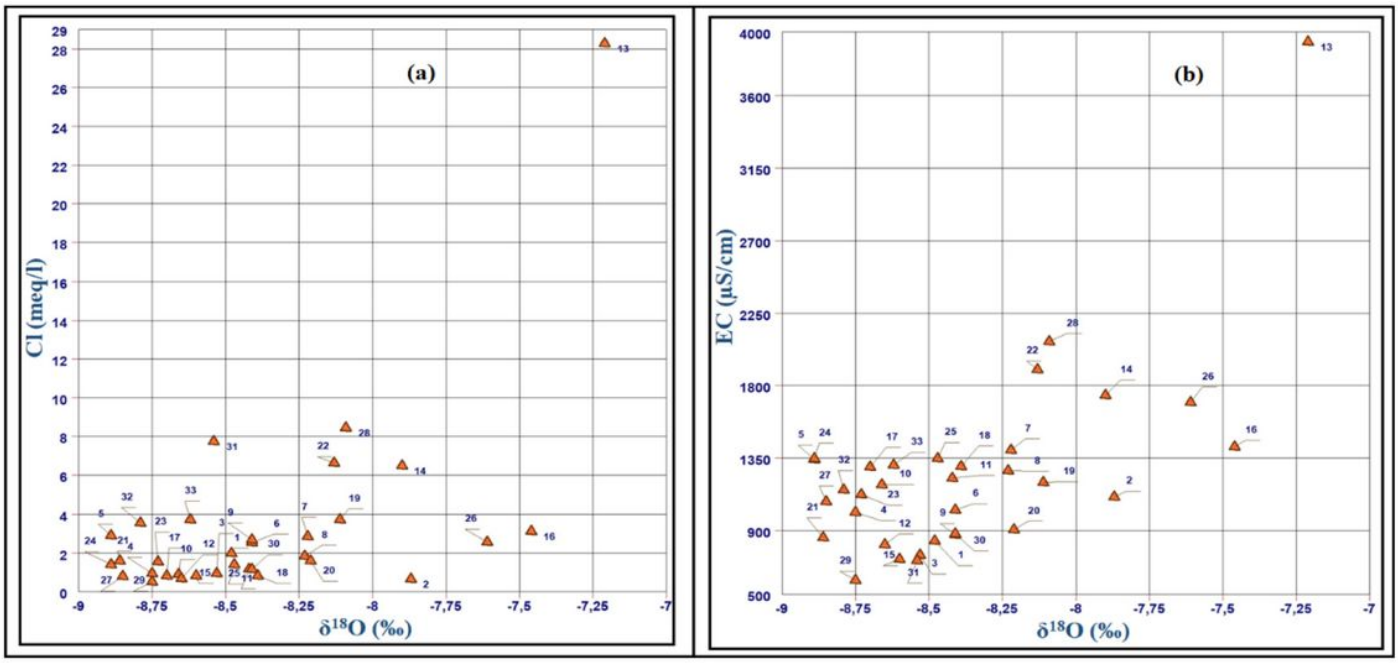


Figure 13

Cl- (meq / l) vs. δ18O (‰) plot (a) and EC (µS / cm) vs. δ18O (‰) of groundwater samples in the study area.

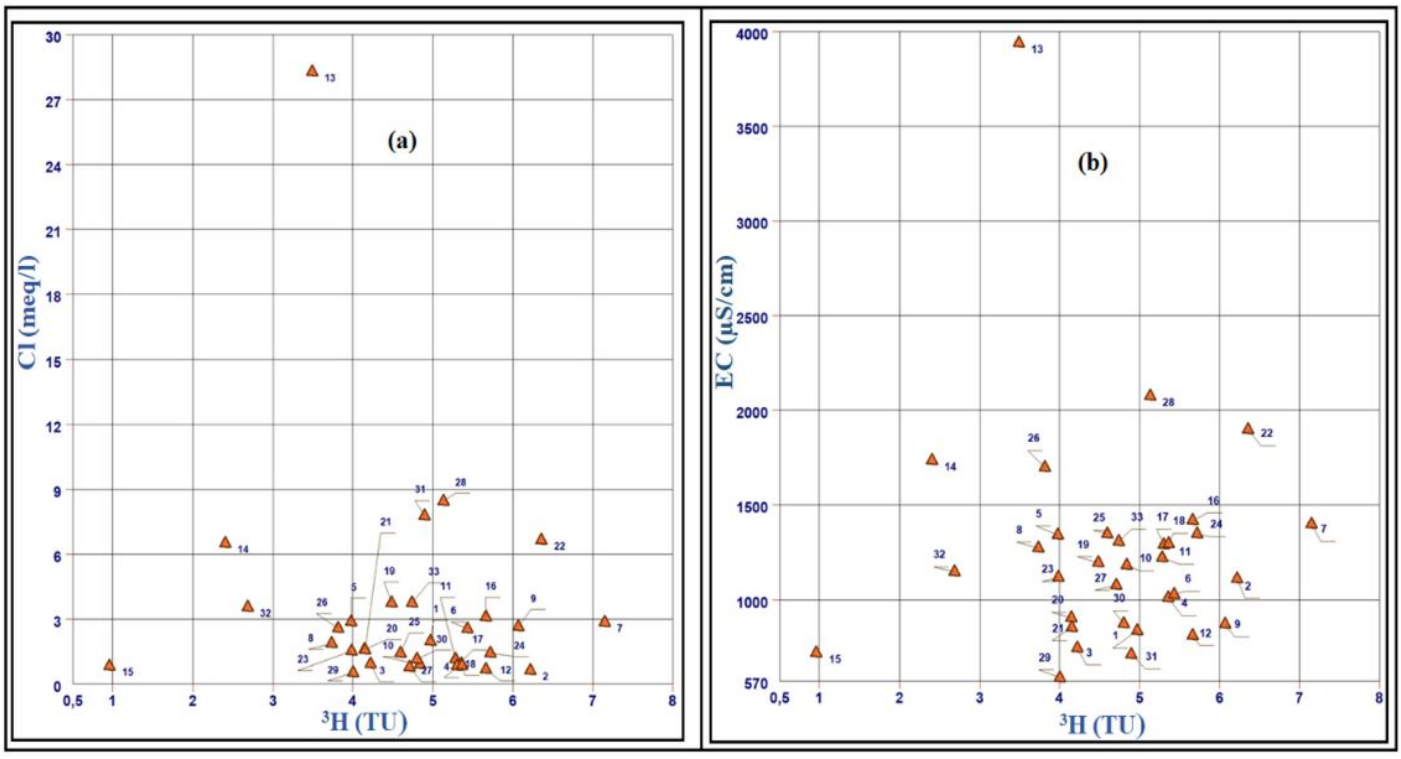


Figure 14

Cl- (meq/l) vs. 3H plot (a) and EC (µS/cm) vs. 3H